Seasonal Differences in the Stationary Response of a Linearized Primitive Equation Model: Prospects for Long-Range Weather Forecasting?

J. D. OPSTEEGH AND H. M. VAN DEN DOOL

Royal Netherlands Meteorological Institute, De Bilt, The Netherlands

(Manuscript received 23 April 1980, in final form 30 June 1980)

ABSTRACT

A linear steady-state primitive equation model has been developed for the computation of stationary atmospheric waves that are forced by anomalies in surface conditions. The model has two levels in the vertical. In the zonal direction the variables are represented by Fourier series, while in the meridional direction a grid-point representation is used. The equations governing atmospheric motion are linearized around a zonally symmetric state which depends on latitude and height according to Oort (1980).

We have studied the amplitude and phase relations of the model response as a function of latitude for a very simple heating, which is sinusoidal in the zonal direction, with zonal wavenumber m (m = 1, 10) and constant in the meridional direction, using February mean conditions.

The response of the model indicates that a heating in the tropics can have a substantial influence on the middle and high latitudes, provided that part of the heating is in the westerlies. We have compared the model response for such a heating with the results of similar experiments with GCM and a linear barotropic model and also with mean anomaly patterns at middle and high latitudes derived from observations for Northern Hemispheric winters with a warm equatorial Pacific. In all cases we find strong similarities of hemispheric wave patterns.

We plan to test the model for the prediction of that part of the anomalies in the monthly or seasonal mean circulation that comes from persistent abnormal surface conditions. In order to predict more than a persistent atmospheric response, such an anomaly in the surface conditions must have different effects in different months or seasons. We have tested the hypothesis that due to a changing zonally symmetric state, the response to a prescribed heating will be different in the four seasons. This effect is computed for a heating in the tropics and in the middle latitudes. Both in amplitude and phase the response to exactly the same heating can change significantly from one season to the next.

1. Introduction

The belt of westerlies at middle and high latitudes of the Northern Hemisphere has been documented for a long time. When looking at a sequence of hemispheric streamline maps, large meanders in the predominantly westerly winds become visible. Some of these meanders have a quasi-stationary character. They are clearly seen on maps of the long-term averaged circulation. The nature of these standing waves is often studied by assuming that they arise as a linear atmospheric response to zonal asymmetries in earth surface conditions. This makes it possible to study the standing waves with simple linear steady-state models. Saltzman (1968) has given an extensive analysis of this approach. The response of these models to forcing by the earth orography (Charney and Eliassen, 1949; Sankar Rao, 1965) and the exchange of sensible heat with the earth surface (Smagorinsky, 1953; Döös, 1962) shows good agreement with the observed standing wave pattern.

Until 1968 most of the studies had been performed with analytical methods and, therefore, the model atmosphere had to be further simplified to a quasi-geostrophic β-plane, with a zonally symmetric state that is only dependent on height. Saltzman (1968) suggested incorporating the ageostrophic and nonlinear effects and using a zonally symmetric state which depends on latitude and height according to observations. Webster (1972) and Egger (1976a) presented two-level models based on the primitive equations in which winds can be ageostrophic. Webster applied his model only in the tropics, while Egger (1976b, 1978) simulated the standing wave pattern for January and July for the whole Northern Hemisphere. Recently, Ashe (1979) simulated the standing waves with a nonlinear steady-state model.

In this paper we will present a model similar to the one used by Egger with special emphasis on the prospects of making long-range weather forecasts with these models. From the point of view of a long-range weather forecaster, it would be interesting to know the stationary response caused by local anomalies in earth surface conditions, that is, deviations from their long-term mean value. This makes sense only when we know this anomalous forcing

0022-4928/80/102169-17$08.25

beforehand, for example, in case of persistent anomalies. Persistent anomalies in earth surface conditions are often found in the large-scale distribution of the sea surface temperature (SST), which maintains its character for many months. It is often thought that SST anomalies may act as heat sources or sinks, producing anomalies in the circulation pattern of the atmosphere. It has been shown by many authors that there is indeed some statistical relation (Ratcliffe and Murray, 1970; Namias, 1978; Davis, 1978; Harnack and Landsberg, 1978). In various studies with GCM's, efforts were made to simulate and quantify this relation (Houghton *et al.*, 1974; Rowntree, 1976; Huang, 1978). But the response produced by the SST anomalies is generally small and hard to distinguish from the noise in the model statistics caused by the transient weather systems.

Egger (1977) has studied the atmospheric response to SST anomalies with a linear steady-state model. He computed the atmospheric response to a pool of warm water near Newfoundland and found some agreement with surface pressure maps constructed from observations by Ratcliffe and Murray.

The value of such a description, of course, depends very much on the magnitude of the contribution of SST anomalies to anomalies in the mean circulation. There are indications that for middle latitudes most of the variance in the monthly mean circulation can be explained from the transient weather systems (Madden, 1976) and therefore, in general, only a small part is caused by external forcing. This means that only on those occasions when SST anomaly distributions give rise to large responses, can the model results be used to predict future weather.

A limitation on the use of a persistent forcing anomaly for prediction purposes might be that only persistent anomalies in the circulation are produced. In that case the model predicts persistence. However, the zonally symmetric component of the circulation shows important changes from one month to the next. Therefore, due to interaction with the zonally symmetric flow it is likely that persistent heating will have a different effect in different months or seasons.

The model described in this paper has two levels and is based on the primitive equations. It is linearized around a zonally symmetric state that depends on height and latitude according to Oort (1980). The zonal symmetry allows us to expand the model variables in Fourier series along latitude circles; a forcing in zonal wavenumber m leads to a model response in zonal wavenumber m only. In the meridional direction a grid-point representation is used with 23 points between the equator and the pole. The heating is prescribed at the intermediate atmospheric level. To obtain a clear picture of the model response, we will use a prescribed heating rather than an interactive heating scheme.

First, we will describe the results of some experiments to show the behavior of the model for different zonal wavenumbers. The model response to a heating that is sinusoidal in the zonal direction with zonal wavenumber m (m = 1, 10) and an infinite wavelength in the meridional direction is computed. Because the zonal mean winds, the zonal mean temperatures, the zonal mean static stability and the Coriolis parameter are functions of latitude, the amplitude and phase of the resulting disturbances will also depend on latitude. Thus a plot of amplitude and phase against latitude will be the most suitable way of discussing the results for each of the wavenumbers. In a second experiment, we will study the influence of an anomalous heating in the tropics on the atmospheric response in middle latitudes. We try to get a better understanding of this response by comparing the model results with the properties of a quasi-geostrophic model. Finally, the prospects of using this model for the prediction of the anomalous monthly or seasonal mean circulation, caused by persistent SST anomalies, are investigated by testing the hypothesis that a persistent heating will have different effects in different months or seasons. The response of the model is computed for each of the four seasons, using a heating distribution that is the same in each season. We have carried out two experiments, one with a heating in middle-latitudes and one with a heating in the tropics. The differences between the eight model runs are carefully studied.

2. Derivation of the model equations

The model equations can be derived by first applying a time average to the basic laws governing the instantaneous atmosphere. Apart from new unknowns that appear in the momentum and thermodynamic equations as additional forcing and heating, the resulting equations look very much the same as the original ones (Opsteegh and Van den Dool, 1979). In order to construct model equations, we follow roughly the approach by Egger (1976a).

The equations for the monthly mean flow are linearized around a basic state, which is the normal (or long-term) monthly mean circulation. For example,

$$\bar{U} = U_n + \hat{u}, \tag{1}$$

where, $\bar{U}$, U_n and $\hat{u}$ are the monthly mean zonal wind for a particular month, the normal monthly mean zonal wind and the anomalous component. All three quantities depend on latitude, longitude and height.

We now substitute (1) in the equations for the time-averaged quantities and neglect the tendency term and terms nonlinear in $\hat{u}$, $\hat{v}$, etc. Further we subtract from the equations the terms describing the normal monthly mean atmospheric state. We then obtain a set of linear stationary equations in the deviations ($\hat{u}$, $\hat{v}$, etc.). In order to derive tract-

able model equations, the normal flow is divided further into a zonal symmetric and a zonal asymmetric part. For example,

$$U_n = U_{sn} + U_{an}, \tag{2}$$

where U_{sn} and U_{an} are the symmetric and the asymmetric part of the normal zonal wind. After substitution of (2) we get the final anomaly (or perturbation) equations. Because we will not deal in this study with the terms describing the interaction of the perturbations with both the mean meridional flow and the normal standing eddies, we transfer these terms to the right-hand side of the perturbation equations. The equations are expressed in curvilinear coordinates with pressure as the vertical coordinate. They read as follows:

ZONAL MOMENTUM BALANCE

$$U_{sn}\frac{\partial \hat{u}}{\partial x} + \hat{v}\frac{\partial U_{sn}}{\partial y} + \hat{\omega}\frac{\partial U_{sn}}{\partial p} - f\hat{v} + \frac{\partial \hat{\Phi}}{\partial x} - U_{sn}\hat{v}\frac{\tan\varphi}{a} - \hat{F}_{Wx} = \hat{F}_{Ex} - \widehat{MU} - \widehat{SU} \tag{3}$$

MERIDIONAL MOMENTUM BALANCE

$$U_{sn}\frac{\partial \hat{v}}{\partial x} + f\hat{u} + \frac{\partial \hat{\Phi}}{\partial y} + 2U_{sn}\hat{u}\frac{\tan\varphi}{a} - \hat{F}_{Wy} = \hat{F}_{Ey} - \widehat{MV} - \widehat{SV} \tag{4}$$

FIRST LAW OF THERMODYNAMICS

$$U_{sn}\frac{\partial \hat{T}}{\partial x} + \hat{v}\frac{\partial T_{sn}}{\partial y} - \sigma_{sn}\hat{\omega} = \frac{\hat{Q}}{c_p} + \hat{Q}_E - \widehat{MT} - \widehat{ST}. \tag{5}$$

CONTINUITY EQUATION

$$\frac{\partial \hat{u}}{\partial x} + \frac{\partial \hat{v}\cos\varphi}{\cos\varphi\partial y} + \frac{\partial \hat{\omega}}{\partial p} = 0. \tag{6}$$

HYDROSTATIC APPROXIMATION

$$\frac{\partial \hat{\Phi}}{\partial p} = -\hat{\alpha}. \tag{7}$$

EQUATION OF STATE

$$p\hat{\alpha} = R\hat{T}. \tag{8}$$

In the above $\partial x \equiv a\cos\varphi\partial\lambda$ and $\partial y \equiv a\partial\varphi$. The symbols $u, v, \omega, x, y, p, f, \Phi, T, \alpha$ and R have their conventional meaning. $\hat{F}_{Wx}$ and $\hat{F}_{Wy}$ are the dissipation terms and will be specified below. $\hat{F}_{Ex}$, $\hat{F}_{Ey}$ and $\hat{Q}_E$ are the internal eddy sources of momentum and heat. $\widehat{MU}$, $\widehat{MV}$ and $\widehat{MT}$ describe the interaction of the perturbations with the mean meridional flow. $\widehat{SU}$, $\widehat{SV}$ and $\widehat{ST}$ describe the interaction with the normal standing eddies. Of all the terms on the right-hand sides only the anomalous diabatic heating $\hat{Q}/c_p$ will be retained. In this study the heating, which drives the model, will be prescribed.

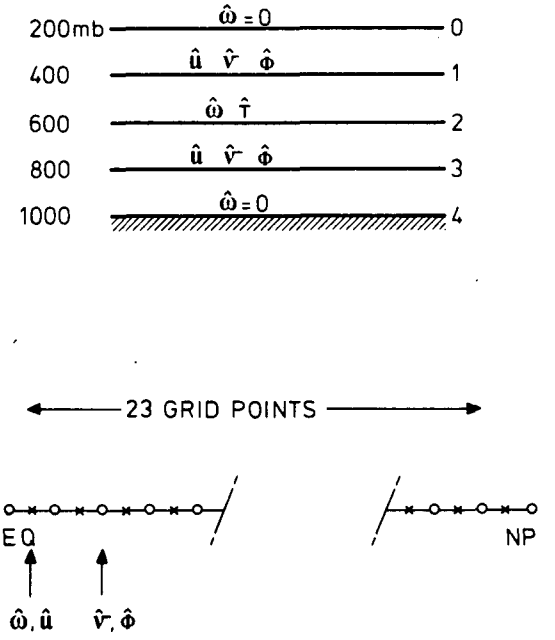

FIG. 1. Discretization of the two-level model in the vertical (upper part) and in the meridional direction (lower part).

a. Vertical discretization

The vertical discretization of the model is shown in the upper part of Fig. 1. The momentum and continuity equations are applied at level 1 (400 mb) and 3 (800 mb), while the thermodynamic equation is applied at level 2 (600 mb). In the last equation $\hat{T}_2$ is eliminated and expressed in $\hat{\Phi}_1$ and $\hat{\Phi}_3$, with the hydrostatic equations and the equation of state. The boundary condition at levels 0 and 4 is

$$\hat{\omega} = 0. \tag{9}$$

By using a rigid top at the tropopause, the propagation of the waves into the stratosphere is prevented. This may cause spurious reflection of wave energy, which affect amplitude and phase of the response in the troposphere (Shutts, 1978; Laprise, 1978).

We now have a set of seven equations in the seven variables $\hat{u}_1, \hat{u}_3, \hat{v}_1, \hat{v}_3, \hat{\Phi}_1, \hat{\Phi}_3$ and $\hat{\omega}_2$. For the friction terms Egger's (1976a) approach is followed. Thus at level 3 we have surface friction and vertical diffusion, while at level 1 there is only vertical diffusion. In the zonal momentum equations they have the form

$$\hat{F}_{Wx3} = K_D(\hat{u}_1 - \hat{u}_3) - K_W\hat{u}_3, \tag{10}$$

$$\hat{F}_{Wx1} = -K_D(\hat{u}_1 - \hat{u}_3), \tag{11}$$

where K_D and K_W are the vertical diffusion and surface friction coefficients, respectively. They are constants in the model. The friction terms in the meridional momentum equations are obtained by replacing $\hat{u}_1$ and $\hat{u}_3$ by $\hat{v}_1$ and $\hat{v}_3$ in (10) and (11).

b. Horizontal discretization

The various terms in the seven model equations contain coefficients that do not depend on longitude. Therefore the perturbation quantities are expanded in Fourier series along latitude circles. In the meridional direction we have chosen a grid-point representation, with 23 grid points between pole and equator. As an example of the Fourier expansion, we write

$$\hat{u}_1 = \sum_{m=1}^{N} \hat{u}_{1m}(\varphi)e^{-im\lambda}, \tag{12}$$

where $\hat{u}_{1m}$ is a complex coefficient. By substitution of these relations into the model equations we get new equations for the complex Fourier coefficients. These equations are given in Appendix A. Finally, we have N sets of 14 linear first-order differential equations for the real and imaginary parts of the Fourier coefficients.

The equations are solved on the grid that is shown in the lower parts of Fig. 1. There are 23 grid points, indicated as crosses with grid distance of slightly less than 4°. $\hat{v}$ and $\hat{\Phi}$ are formulated at intermediate points, indicated with open circles. The boundary conditions are

$$\left.\begin{aligned} \hat{v}\cos(\varphi) &= 0, \quad \varphi = \pi/2 \\ \frac{\partial\hat{\Phi}}{\partial\varphi} &= 0, \quad \varphi = 0 \end{aligned}\right\}. \tag{13}$$

Here $\hat{v}\cos\varphi$ is a variable which is used in the model, instead of $\hat{v}$; it is zero at the pole. At the equator we use a symmetry condition. Some of our experiments have been repeated with the boundary conditions used by Egger (1976a), with almost the same results.

3. Behavior of the model in the zonal wavenumber domain

In order to investigate the characteristic behavior of the model, we solve the system of equations for a heating distribution that is sinusoidal in the zonal direction and constant in the meridional direction. Hence

$$\hat{Q}_2/c_p = A\cos(m\lambda),$$

with $A = 1 \times 10^{-5}$ K s^{-1}. The model solution is derived separately for zonal wavenumbers from 1 to 10. The zonally symmetric fields U_{sn1}, U_{sn3}, T_{sn1}, T_{sn3} and σ_{sn2} have been computed from the data of Oort (1980), while $(\partial U_{sn}/\partial p)_1$ and $(\partial U_{sn}/\partial p)_3$ are derived from the normal temperature fields by applying the thermal wind relation. In this section we have chosen the February mean conditions. The numerical value of the friction coefficient (K_W) is 2×10^{-7} s^{-1}, which is close to the value taken by Egger (1976a). For the vertical diffusion coefficient (K_D) we have chosen a value of 1×10^{-7} s^{-1}. We have neglected the terms that describe the convergence of the meridians, because in a linear model they generate spurious energy. This is outlined in Appendix B.

Most of the experiments with steady-state models have been performed on a β plane, with zonally symmetric fields that are independent of latitude. As a consequence, the forced wave will have the same wavelength in the zonal and meridional directions as the heating wave. In the present model the zonally symmetric state and the derivative of the Coriolis parameter are functions of latitude. Therefore, a heating with wavenumber (m,n) will create a response with the same zonal wavenumber m, but with a complex meridional structure.

As an example we will discuss at some length the geopotential height response in $m = 2$. In the left part of Fig. 2 the horizontal distribution of the geopotential height of 400 and 800 mb is shown. Units are decameters. Because of the symmetry and periodicity of the solution we show only 90° of geographical longitude. In this area the cosine bell-shaped heating is 1×10^{-5} K s^{-1} at $\lambda = 0°$ and 0 at $\lambda = -45°$ and $+45°$. At 800 mb low pressure is found everywhere over the heating in the subtropics, whereas at 70° N the low pressure is observed downstream of the maximum of the heating. At 400 mb there is a system of high pressure downstream of the heating maximum at 50° N. The upstream low-pressure system has an extension to the high northern latitudes.

In the right part of Fig. 2 the same responses are represented in a more informative and concise way: amplitude and phase are plotted as a function of latitude. The amplitude is in meters and the phase in degrees of the wavelength in question (-180 to $+180$). The phase measures the distance of the geopotential ridge to the maximum of the heating. The phase is positive (negative) if the geopotential ridge is found to the east (west) of the heating maximum. It is clear that amplitude and phase show a remarkable dependence on latitude although the heating is the same everywhere. The reason is the latitude-dependence of U_{sn}, T_{sn}, σ_{sn} and β $(=df/dy)$.

Before we discuss amplitude-phase diagrams for all wavenumbers, it should be noted that the resonance wavenumber is very close to $m = 4$ and 5. This wavenumber separates the ultralong waves from the long waves. For the ultralong waves the β term in the vorticity equation dominates over the advective terms, while the opposite is true for the long waves (see, e.g., Saltzman, 1965). In Fig. 3 the geopotential height responses are shown for $m = 1$,

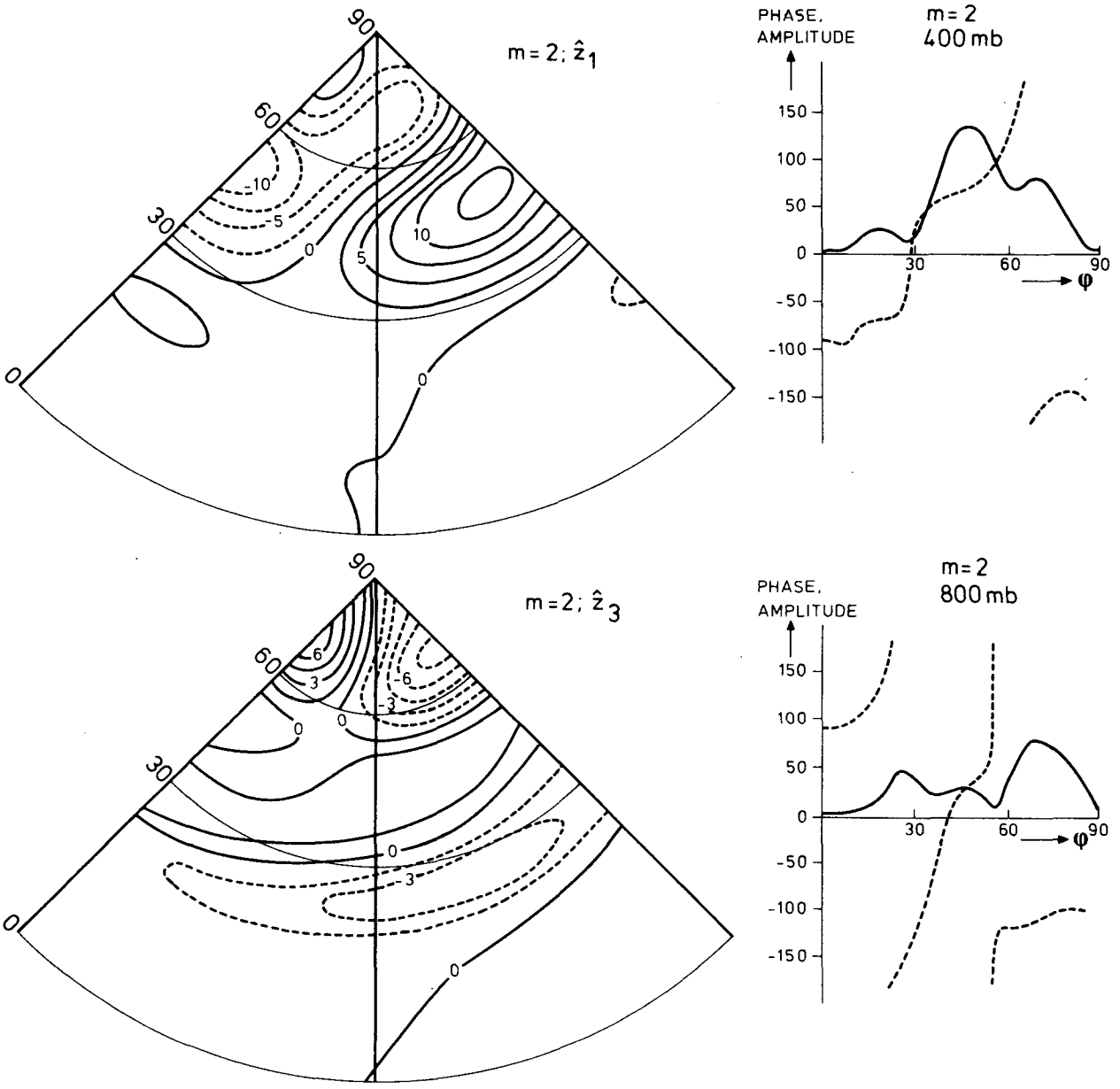

FIG. 2. The geopotential height response of the model at 400 and 800 mb to a heating that is sinusoidal in longitudinal direction (zonal wavenumber 2) and uniform with latitude. The amplitude of the heating is 10^{-5} K s^{-1}. In the left part the response is presented as a geographical distribution, while in the right part amplitude and phase are plotted against latitude. The heating reaches its maximum at $\lambda = 0°$, while at $\lambda = +45°$ and $-45°$ it is zero. A positive phase of the geopotential height means that its maximum is found to the east of the maximum of the heating (at $\lambda = 0$).

2 and 3 (ultralong waves), $m = 4$ and 5 (near-resonance) and $m = 8$ (long wave). The results are complicated but some general features can be seen in Fig. 3.

In the tropical belt of easterlies the amplitudes are very small for all wavenumbers. The heating (cooling) is almost completely balanced by strong upward (downward) motion, while horizontal temperature advection is negligible. This thermally direct circulation was also found by Webster (1972).

In subtropical regions the amplitudes and phase of the ultralong waves increase very fast north of the latitude of zero mean wind. The phase of the subtropical maximum at 800 mb is ~180°, which means that for $m = 1$, 2 and 3 the troughs are found over the heating; the phase of the maximum at 400 mb varies between −70 and −30°.

Going north to the midlatitudes, the amplitude and phase are different for the first three wavenumbers. Nevertheless, looking at the maxima, we

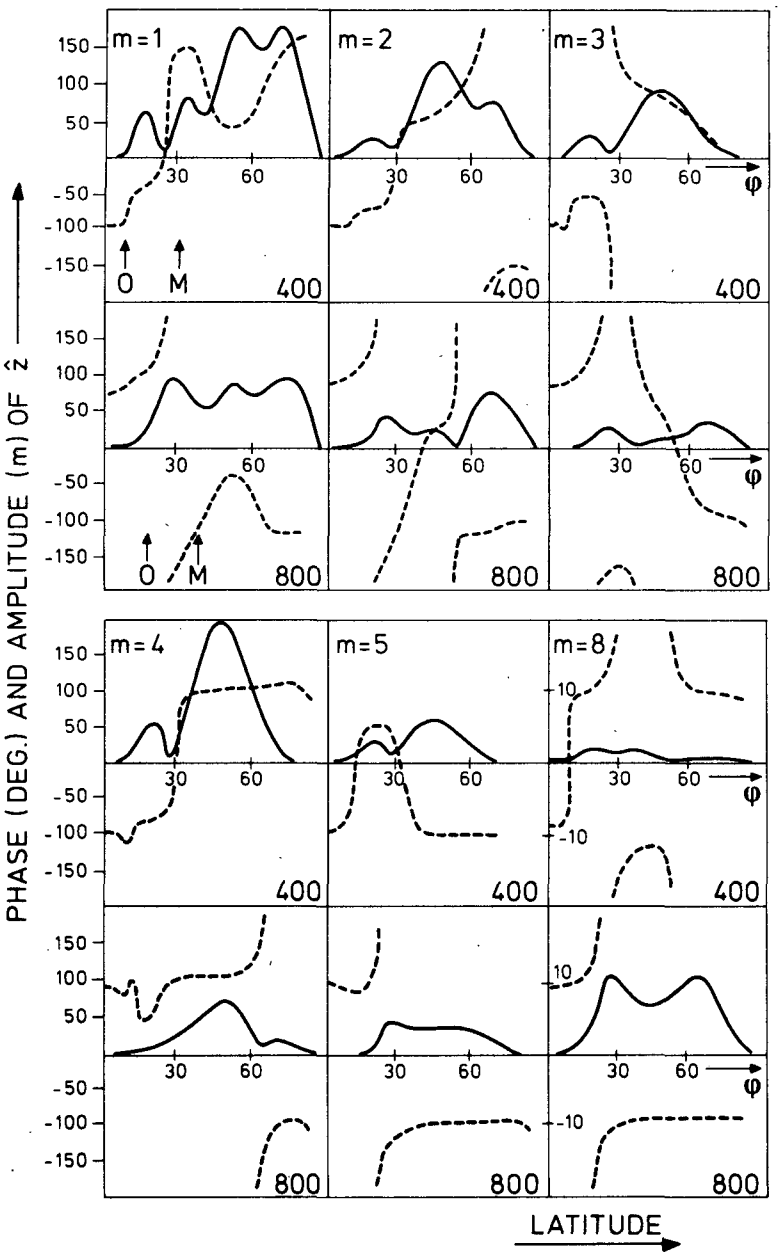

FIG. 3. Amplitude and phase of the geopotential height response at 400 and 800 mb as a function of latitude and wavenumber. The heating has zonal wavenumber m (m = 1, 2, 3, 4, 5 and 8) and infinite meridional wavelength; the amplitude is 1×10^{-5} K s^{-1} for all m. The latitudes where the mean wind is zero (0) and where it reaches its maximum (M) are indicated by arrows in the graph of m = 1. The vertical scales of amplitude (gpm) and phase (deg) are the same except for m = 8, where a different scale for the amplitude had to be used.

find the same general picture that can be derived from experiments with quasi-geostrophic models; at 800 (400) mb a high is found upstream (downstream) of the heating.

For infinite meridional wavelength of the heating, wavenumbers 4 and 5 are close to resonance. They exhibit a quite different behavior than the ultralong waves. The smooth decrease of amplitude with wavenumber is interrupted at m = 4.

As a representative of the long wave we have chosen m = 8. The most prominent feature in its response is that the amplitude is at least one order of magnitude smaller than that of the ultralong waves. (Note the difference in vertical scale for m = 8.)

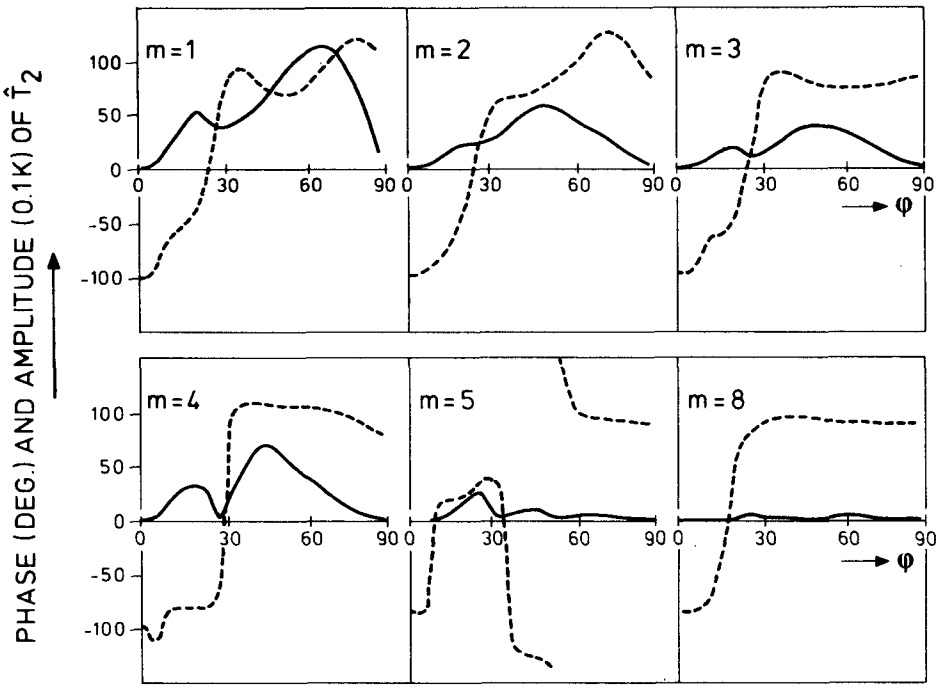

FIG. 4. As in Fig. 3, but now for the temperature response at 600 mb. The vertical scales for the phase (degrees) and temperature (0.1 K) are the same.

The height response at 400 and 800 mb, of course, can be combined into a temperature response at 600 mb. In Fig. 4 amplitude-phase diagrams are shown for $\hat{T}_2$. Some clear conclusions can be drawn now:

1) The temperature wave can be found downstream of the heating wave. This is perfectly true for $m = 8$, nearly true for $m = 1, 2$ and 3 and only at the resonance wavelength deviations of the simple concept occur.

2) The phase of temperature wave has a bimodel distribution with peaks at $+90°$ and $-90°$. This indicates that the zonal advection of $\hat{T}_2$ by the climatological wind cools the area of maximum diabatic heating ($\hat{Q}/c_p$) as much as possible.

A good impression of the way in which the diabatic heating is balanced is given in Fig. 5. Here we show the value of the three terms in the thermodynamic equation as a function of latitude at the longitude of maximum heating. The sum of the three terms equals the heating that is indicated by the dashed straight line ($\hat{Q}/c_p = 1 \times 10^{-5}$ K s^{-1}). From this figure it is clear that at the very low latitudes the heating is almost completely balanced by vertical motion, whereas temperature advection plays a minor role. This holds for all wavenumbers. For the ultralong waves the advection terms are dominant at middle latitudes. This balance is not very efficient because the zonal temperature advection is counteracted by the meridional temperature advection and the vertical motion term. At many latitudes the latter two processes warm the air, whereas cooling is required in order to oppose the diabatic heating. From the balance in wavenumbers 4 and 5 it can be seen that they are close to resonance. The terms are very large and mainly counteract each other. Wavenumber 8 shows a different picture at midlatitudes. Here the heating is balanced efficiently because all terms have a positive contribution.

To summarize the results, we have found that there is some agreement with the results of studies with a local heating at midlatitudes and in the tropical regions. However, the general picture is much more complicated than can be deduced from local experiments. It turns out that even for a simple heating distribution (heating is kept constant with latitude) the amplitude as well as the phase of the response is strongly dependent on latitude.

4. The influence of heating in the tropics on the standing waves in the middle latitudes

In most of the experiments that have been performed with steady-state models so far, the nature of the standing eddies at midlatitudes has been investigated without the influence of heating in the tropics. However, at present it is not clear how important the heating in the tropics is and whether a steady-state model can handle it properly.

Egger (1977) investigated the influence of an

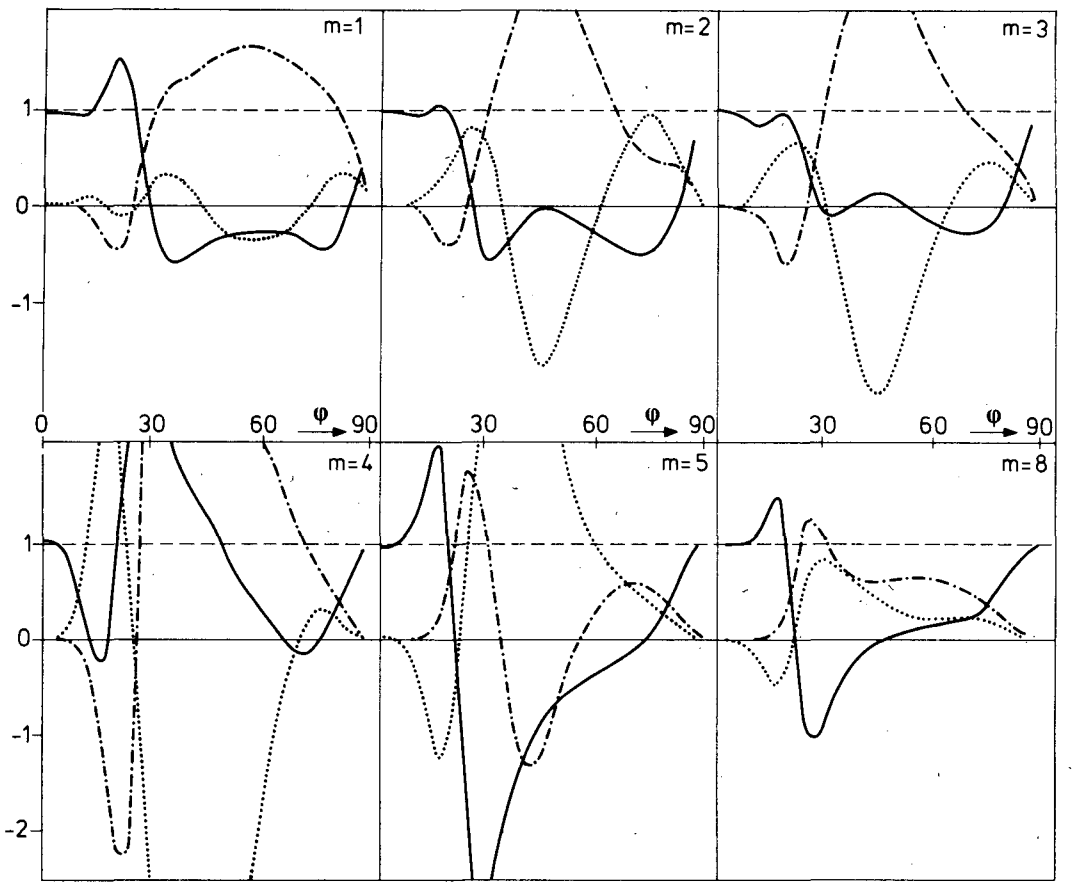

FIG. 5. Thermodynamic balance as a function of latitude at the longitude of maximum heating. The heating is indicated with a dashed line ($\hat{Q}/c_p = 1 \times 10^{-5}$), the vertical motion term with a solid line, the zonal temperature advection with a dashed-dotted line and the meridional advection with a dotted line. Units are 1×10^{-5} K s^{-1}.

anomalous warm region in the tropical Atlantic and the Pacific on the standing eddies in middle latitudes with a steady-state PE model. In the Pacific experiment the heating was restricted to the belt of easterlies, whereas in the Atlantic experiment part of the heating region was situated in the westerlies. The midlatitude response to the heating in the Pacific was negligible, but the warm spot in the Atlantic Ocean results in a significant response, although it is smaller than the one derived with a GCM for the same tropical Atlantic sea surface temperature anomaly (Rowntree, 1976). Egger did not investigate in detail the differences between the two experiments, although he suggested that the critical line where the zonally averaged mean wind changes sign, as well as the equatorial easterlies might have a profound influence on the intensity and position of the standing waves at midlatitudes.

We have made similar experiments with the two-level steady-state PE model. However, in order to get a better understanding of the responses, we will start with a theoretical study of the behavior of the simpler quasi-geostrophic two-level model on a β plane.

a. Response of a quasi-geostrophic model

We now consider tropical heating south of latitude φ_0. North of φ_0 the heating is zero everywhere. Hence at latitudes north of φ_0 the response must be a solution of the homogeneous equations. Stationary Rossby waves are solutions of these homogeneous equations. The question is whether forcing at these low latitudes will excite these waves. In the following we will show how this depends on the zonally symmetric conditions and on the particular value of β and f.

The equations of the quasi-geostrophic two-level model on a β plane are

$$U_{sn1}\frac{\partial^2 \hat{v}_1}{\partial x^2} + U_{sn1}\frac{\partial^2 \hat{v}_1}{\partial y^2} + \beta \hat{v}_1 = \frac{f_0}{2\Delta p}\hat{\omega}_2, \quad (14)$$

$$U_{sn3}\frac{\partial^2 \hat{v}_3}{\partial x^2} + U_{sn3}\frac{\partial^2 \hat{v}_3}{\partial y^2} + \beta \hat{v}_3 = -\frac{f_0}{2\Delta p}\hat{\omega}_2, \quad (15)$$

$$U_{sn1}\hat{v}_3 - U_{sn3}\hat{v}_1 + \frac{2\Delta p\sigma_{sn2}}{f_0}\hat{\omega}_2 = 0, \qquad (16)$$

where (14) and (15) are the vorticity equations applied at 400 and 800 mb, and (16) is the homogeneous thermodynamic equation applied at 600 mb. For simplicity we have replaced the polar coordinates λ and φ by the rectangular coordinates x and y. In order to get tractable equation, $\hat{\omega}_2$ is eliminated from (14) and (15), using (16), while the remaining variables are expanded in Fourier series in x direction as follows:

$$\begin{pmatrix}\hat{v}_1\\ \hat{v}_3\end{pmatrix} = \sum_{m=1}^{M}\begin{pmatrix}\hat{v}_{1m}\\ \hat{v}_{3m}\end{pmatrix}\exp\left(\frac{2\pi}{L}imx\right),$$

where $L = 2\pi a.\cos\varphi$ is the length of the latitude circle and a is the earth radius. The vorticity equations for the mth Fourier component now have the form

$$\frac{\partial^2\hat{v}_{1m}}{\partial y^2} + K_1\hat{v}_{1m} + K_3\hat{v}_{3m} = 0, \qquad (17)$$

$$\frac{\partial^2\hat{v}_{3m}}{\partial y^2} + K_2\hat{v}_{3m} + K_3\hat{v}_{1m} = 0, \qquad (18)$$

where

$$K_1 = \frac{\beta}{U_{sn1}} - \frac{4\pi^2}{L^2}m^2 - \frac{f_0^2}{4\Delta p^2\sigma_{sn2}}\frac{U_{sn3}}{U_{sn1}}, \qquad (19)$$

$$K_2 = \frac{\beta}{U_{sn3}} - \frac{4\pi^2}{L^2}m^2 - \frac{f_0^2}{4\Delta p^2\sigma_{sn2}}\frac{U_{sn1}}{U_{sn3}}, \qquad (20)$$

$$K_3 = \frac{f_0^2}{4\Delta p^2\sigma_{sn2}}. \qquad (21)$$

If a stationary Rossby wave with zonal wavenumber m exists, it is a solution of (17) and (18). Given a set of constants on the β plane ($\beta, f_0, U_{sn1}, U_{sn3}$ and σ_{sn2}), we will investigate for all zonal wavenumbers whether such solutions exist. Hence we look for solutions that are periodic in the y direction:

$$\begin{pmatrix}\hat{v}_{1m}\\ \hat{v}_{3m}\end{pmatrix} = \begin{pmatrix}A_{1m}\\ A_{3m}\end{pmatrix}\exp(iny). \qquad (22)$$

Substitution of (22) in (17) and (18) gives two homogeneous equations in A_{1m} and A_{3m}. These equations have only a nonzero solution if the determinant is zero. That is,

$$(K_1 - n^2)(K_2 - n^2) - K_3^2 = 0,$$

hence

$$2n^2 = (K_1 + K_2) \pm [(K_1 - K_2)^2 + 4K_3^2]. \qquad (23)$$

For positive n^2 (n is real), the solution is periodic in the y direction and stationary Rossby waves with zonal wavenumber m are possible. Once excited, such waves will influence the midlatitudes. When n^2 is negative, n will be complex and one growing plus a decaying exponential solution is obtained. Such solutions can only exist for nonzero boundary conditions, in contrast with the Rossby waves. When the conditions are such that exponential solutions occur, a nonzero perturbation at latitude φ_0, which arises as a result of the forcing south of φ_0, will be damped exponentially. The amplifying branch has zero amplitude because the solution must satisfy the homogeneous boundary condition at the pole ($\hat{v}_m = 0$ at $\varphi = \pi/2$). In this case the midlatitudes will not feel the heating in the tropics. So by investigating (23) in more detail, we are able to gain some insight into the conditions that are favorable for a tropical disturbance to propagate into the midlatitudes.

From (23) it can easily be seen that in case ($K_1 + K_2$) is positive, there is always at least one positive solution of n^2. The only positive contribution to K_1 and K_2 comes from the β term, provided that the mean wind is westerly. So if the β term is positive and large compared to the other two contributions to K_1 and K_2, we will get periodic solutions. On the other hand, if the zonal wavenumber m is large enough, both solutions for n^2 become negative and the forced disturbance at latitude φ_0 will damp exponentially. Hence from a first glance at (23), we can learn that, given a set of local conditions U_{sn1}, U_{sn3}, β, f_0 and σ_{sn2}, we can expect a critical zonal wavenumber m_c. For wavenumbers $< m_c$ the β term dominates and stationary Rossby waves are excited. Wavenumbers larger than m_c will be damped.

We will quantify this qualitative understanding by determining the critical wavenumber for local β-plane conditions at each grid point. So we take the observed February mean condition at a particular grid point, together with the real value of β and f at that point, and assume that they are independent of latitude. Now K_1, K_2 and K_3 are constant and we can determine the solution for m_c from (23).

Fig. 6 shows the critical zonal wavenumber as a function of latitude. In the belt of easterlies, m_c is zero and no stationary Rossby waves exist. Just to the north of the latitude where U_{sn1} changes sign, all wavenumbers have stationary Rossby-wave solutions (the β term is very large and positive). Going to the north, m_c decreases until it reaches a value of approximately 7 at the latitude where U_{sn3} is zero. North of that latitude, again all wavenumbers have stationary Rossby-wave solutions. At midlatitudes zonal wavenumbers higher than 5 will be damped. Only zonal wavenumbers 1 and 2 have stationary Rossby-wave solutions up to the polar regions.

b. Response of the PE model

With this picture in mind, we now turn to the tropical experiment with the two-level PE model.

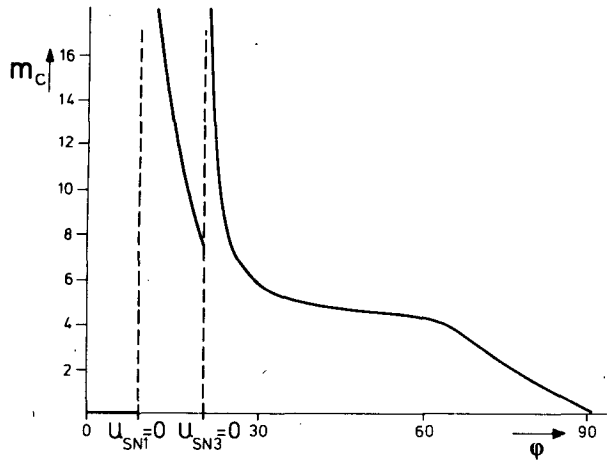

FIG. 6. The critical zonal wavenumber (m_c) as a function of latitude. This wavenumber defines the largest zonal scale that allows periodic solutions in the meridional direction.

We have placed a heating in the tropics with zonal wavenumber m (m = 1, 10), which decreases linearly with latitude. The heating has a maximum at the equator of 1×10^{-5} K s^{-1} and it is zero at 16°N. Fig. 7 shows the response of the model as a function of latitude for m = 1–10 at 400 mb. Friction and vertical diffusion have been excluded in this experiment.

Clearly, wavenumbers 1 and 2 have a periodic solution in the y direction, up to high northern latitudes. Wavenumbers 3, 4 and 5 are damped north of the middle latitudes, while wavenumbers higher than 5 start their damped behavior just north of the subtropics. This is perfectly in agreement with the behavior that was predicted by the critical wavenumber. The amplitudes of the lowest wavenumbers are quite large. However, when friction and vertical diffusion are included, it reduces to a few geopotential decameters.

A major feature of this response, which could not be deduced from our simple analysis of the quasi-geostrophic system, is that the amplitudes increase with increasing latitude. As a consequence, the largest response to a heating in the tropics is found in the polar regions.

From this experiment we draw the conclusion that, even if only linear effects are incorporated, a heating in the tropical regions can have a significant influence on middle and high latitudes, especially when much of the forcing energy is in the low wavenumbers. However, when the heating is situated completely in the belt of easterlies, the disturbance will be damped, according to the critical wavenumber there. This explains the difference in response in Egger's tropical Pacific and Atlantic experiment (Egger, 1977). We are not quite sure yet whether the stationary wave patterns created by our linear model as a response to tropical forcing are realistic in the sense that they can be found also in the response of the real atmosphere or in the results of GCM experiments. We will go into that subject in the next section.

5. The influence of different zonally symmetric states in different seasons

We mentioned in the Introduction that our main interest is in the anomalies that frequently occur in the normal standing wave pattern in a particular

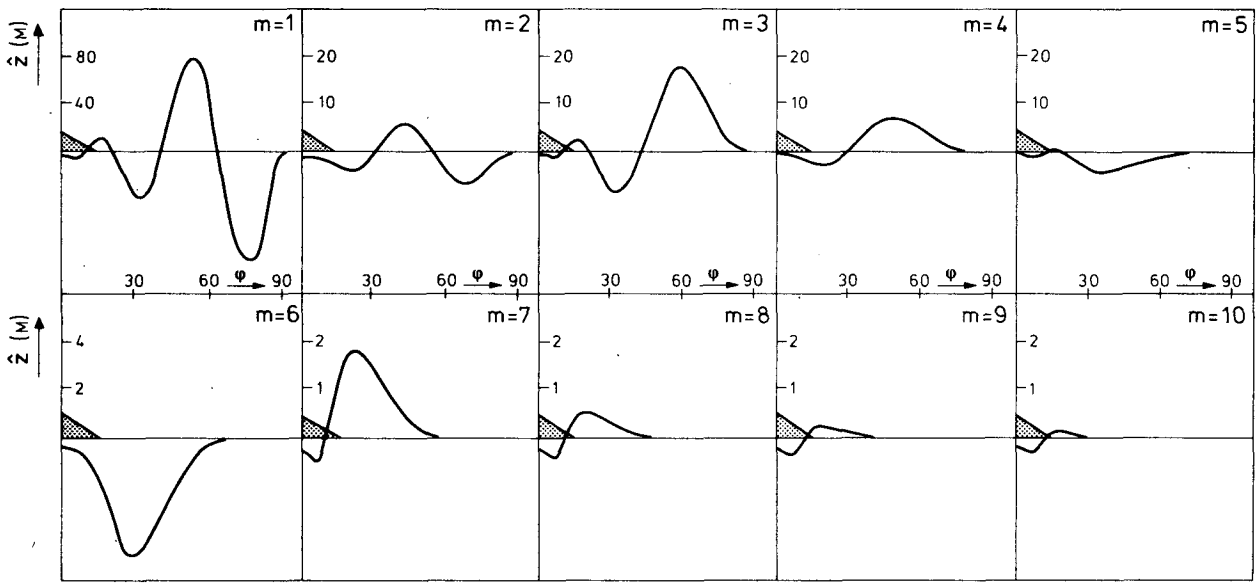

FIG. 7. Geopotential height response at 400 mb for a tropical heating (indicated by the shaded triangle) with zonal wavenumber m = 1, . . . , 10. The amplitude of the height response is given as a function of latitude. The vertical scales are adapted to the magnitude of the amplitude.

month or season. We want to describe these anomalies with a linear steady-state PE model as a response to observed abnormal surface conditions. We have planned to apply the model for the prediction of that part of the anomalous mean circulation that can be explained from the presence of persistent components in the anomalous surface conditions. We have a chance of predicting more than persistence only when these conditions produce a different effect in different months.

Here we demonstrate that due to a changing zonally symmetric state, the response to a prescribed heating differs from season to season. This effect is computed for a rectangular heating of 1×10^{-5} K s^{-1} in middle latitudes and in the tropics. The area enclosed by the heating is 20° latitude and 45° longitude. In this section we discuss all results in the space domain.

a. The tropical heating

Fig. 8 shows the results at 800 mb for the tropical heating. The heating is indicated by the shaded area. Apart from differences in amplitudes and position of the various lows and highs, the overall picture of the response in winter, spring and fall is comparable. However, in summer, the responses in middle and high latitudes are almost zero. Here we can see very clearly the influence of the easterlies. In summer the tropical heating is completely in the zonal belt of easterlies which prevents the excitement of stationary Rossby-Haurwitz waves. The response in the other three seasons in middle latitudes shows low-pressure upstream of the longitude of the heating, while high pressure is found downstream. The most dominant pressure system, however, is the low at high latitudes, ~90° downstream of the longitude of the heating. This low is most intense in spring and fall, with minor phase changes from one season to the other. The low pressure system at midlatitudes is most intense in spring with three separate centers.

b. Comparison with other studies

We have compared the winter response with the results of experiments performed by Rowntree (1976). He computed the mean response of a GCM to the forcing produced by abnormally high SST's during the winter of 1963. The anomaly was in the tropical Atlantic near the Cape Verde Islands, with maximum deviations of 2.7 K. The response as given by Rowntree consists of the signal produced by the SST anomaly plus the noise of the transients. He gives surface pressure anomaly patterns only near the longitudes of the SST anomaly. Low pressure is found over and to the north of the anomaly up to a latitude of about 60°N and high pressure north of that latitude. Our winter response at 800 mb shows a similar pattern. However, we are especially interested in the planetary hemispheric wave structure produced by the GCM. Rowntree gives one hemispheric map of the results at 300 mb. In Fig. 9 his results are compared with our response at 400 mb (in stereographic maps). Of course, the absolute values of the responses cannot be compared, because the magnitude of the atmospheric heating in both experiments is not the same. It turns out that the middle and high latitude wave patterns are very similar. Apparently, a significant part of the anomaly patterns of the GCM can be interpreted in terms of stationary Rossby-Haurwitz waves, arising as a linear atmospheric response to a tropical heating.

Hoskins (1978)[1] computed the steady-state solution of the linear barotropic vorticity equation on the sphere. The tropical SST anomaly was simulated with a negative vorticity source at 300 mb. The computed anomaly pattern at middle and high latitudes has a very strong resemblance to our results at 400 mb. Indeed, the vertical structure of the midlatitude response of the two-level model is nearly equivalent barotropic and the agreement is therefore not surprising.

Very recently Horel and Wallace (1980) computed from observations the mean anomaly pattern at middle and high latitudes for Northern Hemispheric winters in which the sea surface temperatures were above normal in the equatorial Pacific. The resemblance of these hemispheric wave patterns with the abovementioned model results is remarkable. We therefore think that the response of a linear model to a forcing in the tropics is meaningful.

c. The midlatitude heating

Fig. 10 shows the seasonal responses for the middle-latitude heating. Apart from some agreement in the neighborhood of the heated area, the hemispheric wave patterns show very large differences. Downstream of the heating we find a low and upstream a high in all seasons. This downstream low is very strong in summer, when its position is somewhat to the south of the heating center. In winter it is rather weak. The general character of the winter response is a wavenumber 1 wave, although the forcing is distributed over many wavenumbers. This changes completely in spring when higher wavenumbers are present, which results in low and high pressure systems that can hardly be detected in the winter response. For instance in spring the low at (60°N, 120°E) is a dominant system, whereas in winter it is rather weak. The same applies for the low at (40°N, 150°W). The summer responses are very strong, with even higher wavenumbers present. The responses in fall are

[1] Hoskins, B. J., 1978: Horizontal wave propagation on a sphere. *The General Circulation: Theory, Modelling, and Observations*. NCAR Summer 1978 Colloquium, NCAR/CQ-6+1978-ASP, 144–153.

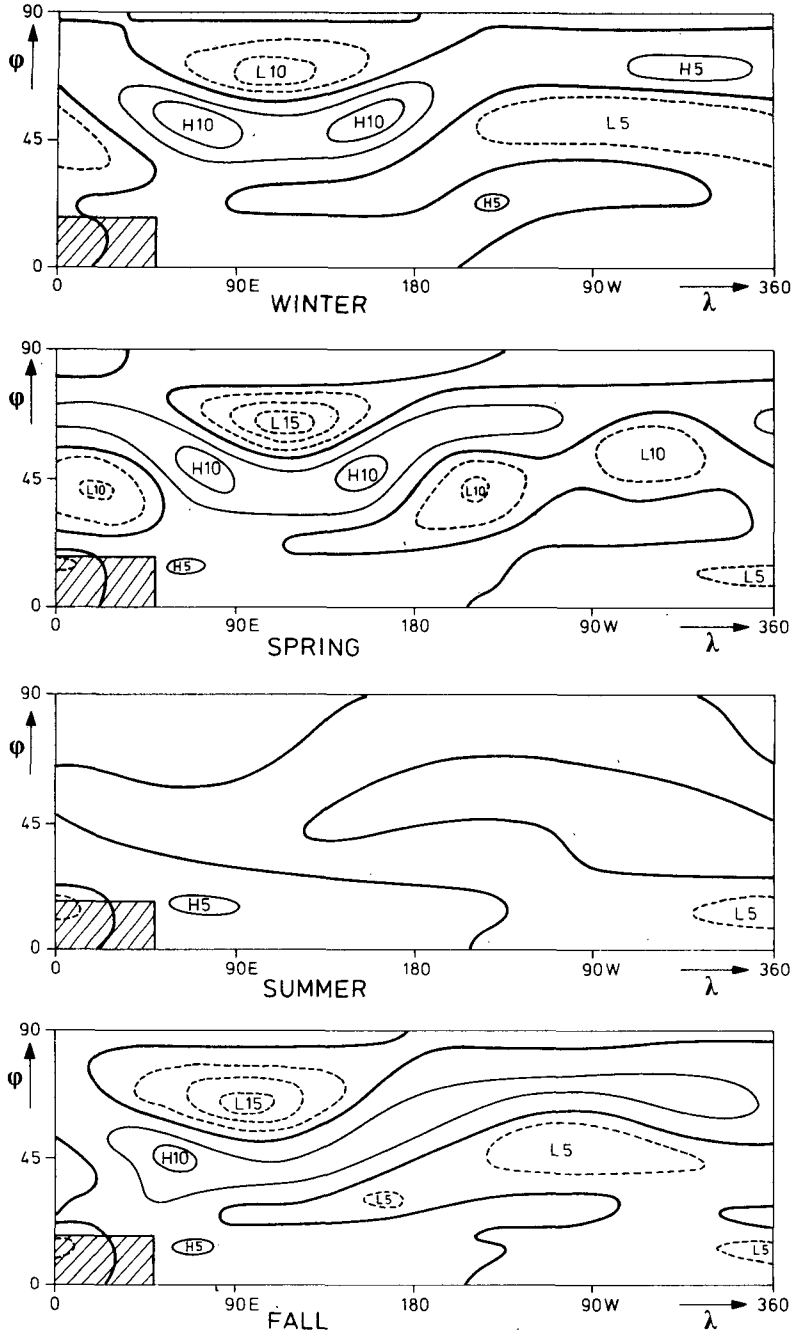

FIG. 8. Geopotential height response (gpm) in four seasons at 800 mb for a rectangular heating of 1×10^5 K s^{-1} in the tropics (shaded area). The net response of the first 10 zonal wavenumbers is given in a geographical display.

dominated again by wavenumber 1. In this season we find low pressure downstream of the heating at all latitudes, whereas in winter this low is flanked by a high at low and high latitudes. The same applies for the upstream high.

The large response in summer is surprising because the strength of the observed anomalies in summer is usually weak compared to those in the other seasons. Also, since the amplitudes of the normal standing eddies are small in summer, part of this discrepancy can possibly be explained by the much weaker heating in summer. The fact that the zonally averaged mean winds are weak in summer is the reason that the model response to a pre-

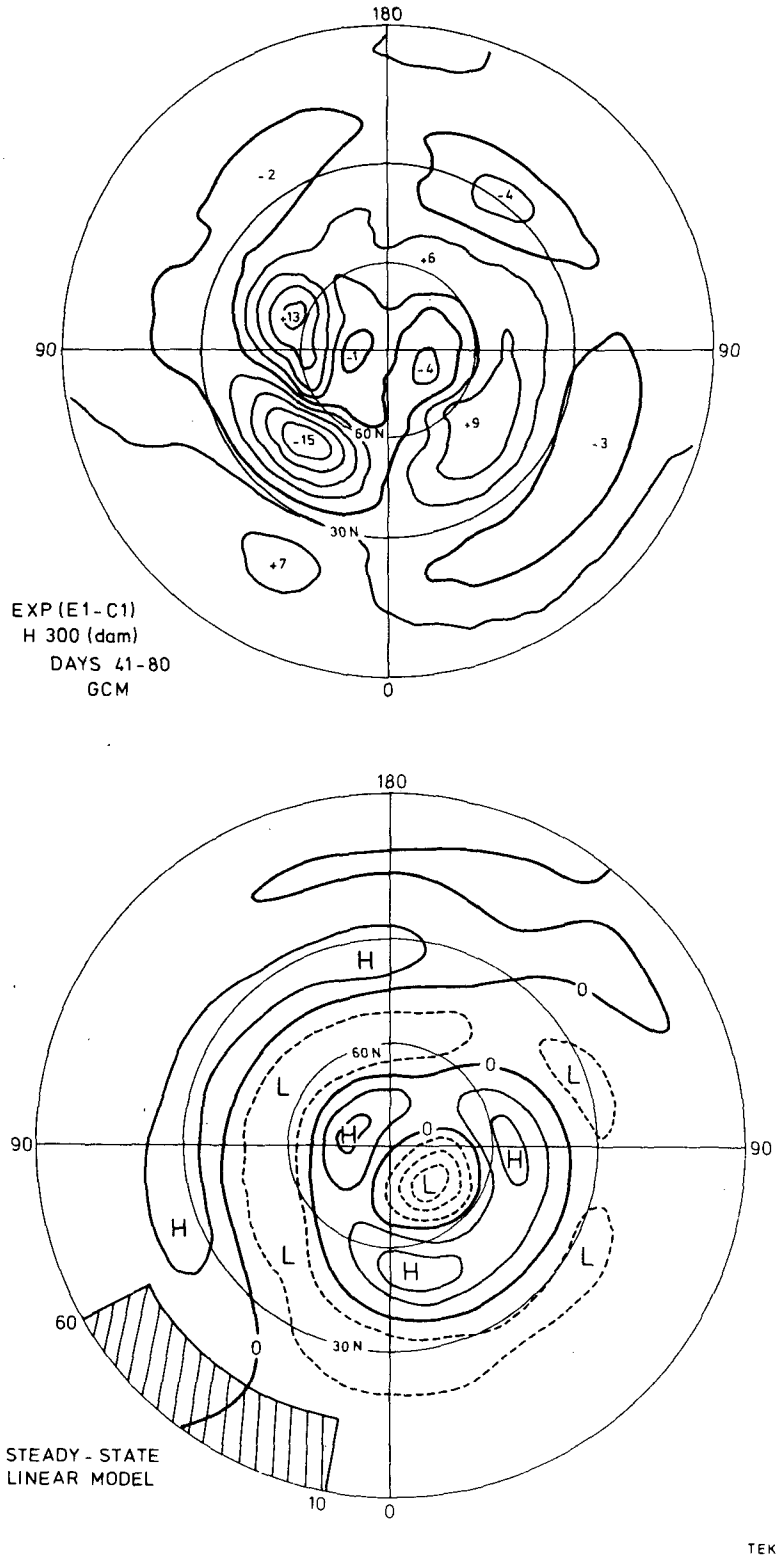

FIG. 9. Geopotential height response at 300 mb of a GCM to a positive SST anomaly in the tropical Atlantic Ocean (Rowntree, 1976) and the steady-state response at 400 mb of the two-level linear model to a similar prescribed heating in the same area. Isopleths are drawn at intervals of 3 and 1 geopotential decameters for the GCM and linear model respectively.

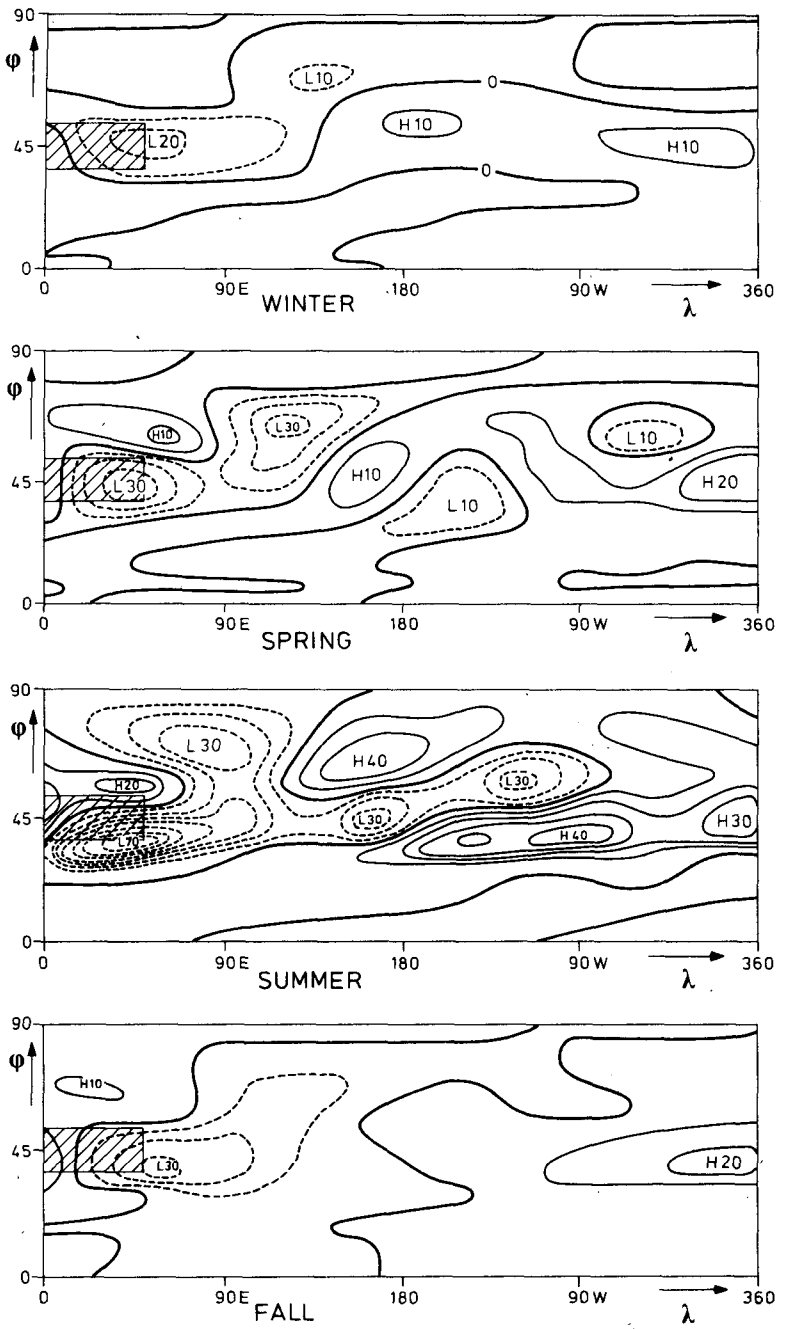

FIG. 10. As in Fig. 8 except for a rectangular heating in the midlatitudes.

scribed heating are large. However, it is likely that for large responses nonlinear processes will have to be considered.

We have shown that if only a changing zonally symmetric mean state is considered, a prescribed heating will have a different response in different seasons. Furthermore, we have shown that the region where we have to specify the heating is larger in winter than in summer. Processes that might influence the response and have not been considered here are, among other things, the interaction of the perturbations with the standing waves (which are different in each season) and the fact that the same anomaly in the surface boundary conditions will certainly cause a different atmospheric heating in different seasons.

6. Discussion

Linear steady-state models have proved to be useful for the description of the normal standing eddies forced by zonally asymmetric surface con-

ditions. Egger (1977) argued that the assumption of linearity would be even better if one is interested in the relatively small anomalies from the normal standing wave pattern in a particular month or season. We have shown that the linear steady-state response to a prescribed anomalous heating distribution is different from one season to the other; therefore, we have a possibility of using such a model for the prediction of that part of the anomalies in the mean circulation that comes from persistent abnormal surface conditions.

Egger (1977) computed the linear steady-state response for an SST anomaly near Newfoundland using January mean conditions. He found some agreement with surface pressure maps constructed by Ratcliffe and Murray (1970) from observations. The very crude approach that Egger used can be improved in many ways. The most obvious thing to do seems the incorporation of the entire geographical distribution of persistent abnormal surface conditions, instead of one anomalous region in the Atlantic Ocean. We have shown in Section 5 that an anomalous heating in the tropics can have significant effects on the circulation in middle and high latitudes, unless it is situated south of the zero mean wind line. This probably means that it is sufficient to deal only with anomalous forcing in the westerlies of the Northern Hemisphere. Apart from SST anomalies, one can think of incorporating the effects of anomalous snow cover or anomalies in sea ice conditions.

A second improvement is the use of heating schemes for the computation of atmospheric heating due to anomalies in the surface conditions, instead of prescribing the heating as we have done in this paper. Döös (1962) showed that the inclusion of atmospheric feedback mechanisms in such a heating scheme is very important, both for the amplitude and for the phase of the resulting atmospheric pressure systems. An example of a heating scheme that is probably appropriate for this purpose is the one used by Vernekar and Chang (1978).

Other improvements, although probably difficult to accomplish, are the incorporation of the interaction of the anomalies with 1) the normal standing eddies and 2) the mean meridional flow and the use of a friction coefficient that differs for land and sea. It would also be interesting to compute the contribution that arises from the anomalous internal forcing (caused by transients). This part of the response is considered unpredictable. In doing so, we will get an impression of the relative importance of the response produced by persistent abnormal surface conditions (signal-to-noise ratio). It will be interesting to compare such signal-to-noise-ratio estimates with those computed in a completely different way by Madden (1976).

We have planned to develop our model along these lines and will next investigate its potential value for the prediction of anomalies in the time-mean circulation. We think that this approach will lead at least to a better understanding of the statistical relations between abnormal surface conditions and future weather, which are presently in use in weather services. These statistical rules indeed have some skill (Nap *et al.*, 1980). If the statistical methods are replaced by a dynamical model of the kind described in this paper, the skill of long-range weather forecasts can perhaps be improved.

Acknowledgement. We thank our colleagues for the stimulating discussions we had during the course of this study. We also thank Mrs. A. Krabman for typing the manuscript. We finally thank the reviewers for their useful suggestions.

APPENDIX A

The Model Equations

ZONAL MOMENTUM BALANCE AT LEVEL 1

$$-\frac{imU_{sn1}}{a\cos\varphi}\hat{u}_{1m}+\frac{\partial U_{sn1}}{a\partial\varphi}\hat{v}_{1m}+\left(\frac{\partial U_{sn}}{\partial p}\right)_1\frac{\hat{\omega}_{2m}}{2}-f\hat{v}_{1m},$$

$$-\frac{im\Phi_{1m}}{a\cos\varphi}-U_{sn1}\frac{\tan\varphi}{a}\hat{v}_{1m}+K_D(\hat{u}_{1m}-\hat{u}_{3m})=0. \quad \text{(A1)}$$

ZONAL MOMENTUM BALANCE AT LEVEL 3

$$-\frac{imU_{sn3}}{a\cos\varphi}\hat{u}_{3m}+\frac{\partial U_{sn3}}{a\partial\varphi}\hat{v}_{3m}+\left(\frac{\partial U_{sn}}{\partial p}\right)_3\frac{\hat{\omega}_{2m}}{2}-f\hat{v}_{3m}-\frac{im\hat{\Phi}_{3m}}{a\cos\varphi}-U_{sn3}\frac{\tan\varphi}{a}\hat{v}_{3m}-K_D(\hat{u}_{1m}-\hat{u}_{3m})+K_w\hat{u}_{3m}=0. \quad \text{(A2)}$$

MERIDIONAL MOMENTUM BALANCE AT LEVEL 1

$$-\frac{imU_{sn1}}{a\cos\varphi}\hat{v}_{1m}+f\hat{u}_{1m}+\frac{\partial\hat{\Phi}_{1m}}{a\partial\varphi}+2U_{2n1}\frac{\tan\varphi}{a}\hat{u}_{1m}+K_D(\hat{v}_{1m}-\hat{v}_{3m})=0. \quad \text{(A3)}$$

MERIDIONAL MOMENTUM BALANCE AT LEVEL 3

$$-\frac{imU_{sn3}}{a\cos\varphi}\hat{v}_{3m}+f\hat{u}_{3m}+\frac{\partial\hat{\Phi}_{3m}}{a\partial\varphi}+2U_{sn3}\frac{\tan\varphi}{a}\hat{u}_{3m}-K_D(\hat{v}_{1m}-\hat{v}_{3m})+K_w\hat{v}_{3m}=0. \quad \text{(A4)}$$

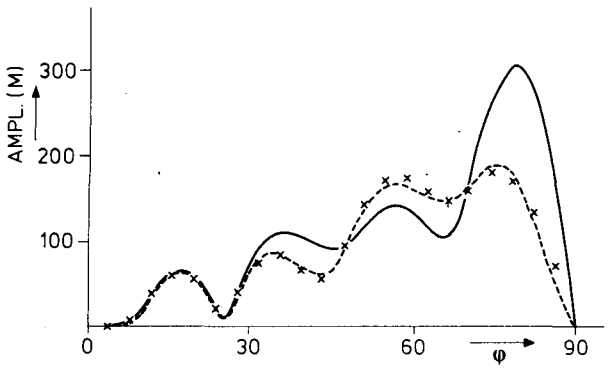

FIG. B1. Amplitude of the geopotential height at 400 mb as a function of latitude. The heating is sinusoidal in longitudinal direction ($m = 1$) and uniform with latitude. Three experiments can be distinguished: (1) convergence terms included (solid line), (2) convergence terms dropped (crosses) and (3) modified convergence terms (dashed line).

THERMODYNAMIC BALANCE AT LEVEL 2

$$\frac{imp_2U_{sn2}}{2R\Delta pa\cos\varphi}(\hat{\Phi}_{3m}-\hat{\Phi}_{1m})+\frac{\partial T_{sn2}}{a\partial\varphi}\left(\frac{\hat{v}_{1m}+\hat{v}_{3m}}{2}\right)-\sigma_{sn2}\hat{\omega}_{2m}-\hat{Q}_{2m}/c_p=0. \quad \text{(A5)}$$

Here p_2 and Δp are 600 and 200 mb, respectively.

CONTINUITY EQUATION AT LEVEL 1

$$-\frac{im\hat{u}_{1m}}{a\cos\varphi}+\frac{\partial(\hat{v}_{1m}\cos\varphi)}{a\cos\partial\varphi}+\frac{\hat{\omega}_{2m}}{2\Delta p}=0. \quad \text{(A6)}$$

CONTINUITY EQUATION AT LEVEL 3

$$-\frac{im\hat{u}_{3m}}{a\cos\varphi}+\frac{\partial(\hat{v}_{3m}\cos\varphi)}{a\cos\varphi\partial\varphi}-\frac{\hat{\omega}_{2m}}{2\Delta p}=0. \quad \text{(A7)}$$

These seven equations have been reduced to four by eliminating $\hat{u}$ and $\hat{\omega}$ by substitution of (A5) to (A7) in (A1) to (A4). Expressed in the real and imaginary parts of the mth Fourier coefficients we finally have N sets of eight equations. The equations can be solved by discretization of the differential equations and inverting the matrix of the resulting system of linear equations.

APPENDIX B

Terms Related to the Convergence of the Meridians

The terms related to the convergence of the meridians appear in the momentum equation as nonlinear terms:

$$\left.\begin{aligned}\frac{\partial u}{\partial t}&=\frac{uv\tan\varphi}{a}+\cdots\\ \frac{\partial v}{\partial t}&=-\frac{u^2\tan\varphi}{a}+\cdots\end{aligned}\right\}. \quad \text{(B1)}$$

So they have to be linearized in the model

$$\left.\begin{aligned}\frac{\partial\hat{u}}{\partial t}&=\frac{U_{sn}\hat{v}\tan\varphi}{a}+\cdots\\ \frac{\partial\hat{v}}{\partial t}&=\frac{-2U_{sn}\hat{u}\tan\varphi}{a}+\cdots\end{aligned}\right\}. \quad \text{(B2)}$$

When the kinetic energy equation is formed by adding $\hat{u}\partial\hat{u}/\partial t$ and $\hat{v}\partial\hat{v}/\partial t$ it can easily be seen that (B2) leads to an extra term: $U_{sn}\hat{u}\hat{v}(\tan\varphi/a)$. Hence the convergence terms may act as a source or sink of kinetic energy. This is an artificial result of the linearization that does not occur in (B1). However, we do not know in advance how serious this energetic inconsistency is for a stationary model ($\partial\hat{u}/\partial t=\partial\hat{v}/\partial t=0$). Therefore, we have performed three experiments. For the heating described in Section 3 we computed the model response with (Exp. 1) and without (Exp. 2) the convergence terms, while in the third experiment (Exp. 3) we retain these terms in such a way that they do not appear anymore in the kinetic energy balance of the perturbations. This can be done by taking half the value of the convergence term in the meridional momentum balance and leaving the term in the zonal momentum balance unaffected.

The differences in the results of the three experiments are very small for the higher wavenumbers. However, for the lower wavenumbers the differences are significant, especially in high latitudes. The amplitudes of the geopotential height for Exp. 1 are very large at high latitudes compared to Exps. 2 and 3. This can be seen in Fig. B1 for wavenumber 1. The figure shows the amplitude of the geopotential height at 400 mb as a function of latitude. The results for Exp. 3 hardly differ from those obtained with Exp. 2, whereas the amplitudes of the response for Exp. 1 are much larger. Apparently, they only have large effects in polar regions when they appear artificially in the perturbation kinetic energy balance. We conclude that it is better to drop these terms altogether.

REFERENCES

Ashe, S., 1979: A nonlinear model of the time-average axially asymmetric flow induced by topography and diabatic heating. *J. Atmos. Sci.*, **36**, 109–126.

Charney, J. G., and A. Eliassen, 1949: A numerical method for predicting the perturbations of the middle latitude westerlies. *Tellus*, **1**, 38–55.

Davis, R. E., 1978: Predictability of sea level pressure anomalies over the North Pacific Ocean. *J. Phys. Oceanogr.*, **8**, 233–246.

Döös, B. R., 1962: The influence of sensible heat with the earth's surface on the planetary flow. *Tellus*, **14**, 133–147.

Egger, J., 1976a: The linear response of a hemispheric two-level primitive equation model to forcing by topography. *Mon. Wea. Rev.*, **104**, 351–363.

——, 1976b: On the theory of steady perturbations in the troposphere. *Tellus*, **28**, 381–389.

——, 1977: On the linear theory of the atmospheric response to sea surface temperature anomalies. *J. Atmos. Sci.*, **34**, 603–614.

——, 1978: On the theory of planetary standing waves: July. *Beitr. Phys. Atmos.*, **51**, 1–14.

Harnack, R. P., and H. E. Landsberg, 1978: Winter season temperature outlooks by objective methods. *J. Geophys. Res.*, **83**, 3601–3616.

Horel, J. D., and J. M. Wallace, 1980: Planetary scale atmospheric phenomena associated with the interannual variability of sea-surface temperature in the Equatorial Pacific. Submitted to *Mon. Wea. Rev.*

Houghton, D. D., J. E. Kutzbach, M. McClintock and D. Suchman, 1974: Response of a general circulation model to a sea temperature perturbation. *J. Atmos. Sci.*, **31**, 857–868.

Huang, J. C. K., 1978: Response of the NCAR general circulation model to North Pacific sea surface temperature anomalies. *J. Atmos. Sci.*, **35**, 1164–1179.

Laprise, R., 1978: On the influence of stratospheric conditions on forced tropospheric waves in a steady-state primitive equation model. *Atmosphere-Ocean*, **16**, 300–314.

Madden, R. A., 1976: Estimates of the natural variability of time-averaged sea level pressure. *Mon. Wea. Rev.*, **104**, 942–952.

Namias, J., 1978: Multiple causes of the North American abnormal winter 1976–1977. *Mon. Wea. Rev.*, **106**, 279–295.

Nap, J. L., H. M. Van den Dool and J. Oerlemans, 1980: A verification of long-range weather forecasts in the seventies. Submitted to *Mon. Wea. Rev.*

Oort, A. H., 1980: Global atmospheric circulation statistics, 1958–1973. NOAA Prof. Pap. (in preparation) [Govt. printing office, Washington, DC].

Opsteegh, J. D., and H. M. Van den Dool, 1979: A diagnostic study of the time-mean atmosphere over northwestern Europe during winter. *J. Atmos. Sci.*, **36**, 1862–1879.

Ratcliffe, R. A. S., and R. Murray, 1970: New lag associations between North Atlantic sea temperature and European pressure applied to long-range weather forecasting. *Quart. J. Roy. Meteor. Soc.*, **96**, 226–246.

Rowntree, P. R., 1976: Response of the atmosphere to a tropical Atlantic Ocean temperature anomaly. *Quart. J. Roy. Meteor. Soc.*, **102**, 607–625.

Saltzman, B., 1965: On the theory of the winter average perturbation in the troposphere and stratosphere. *Mon. Wea. Rev.*, **93**, 195–211.

——, 1968: Surface boundary effects on the general circulation and macroclimate: A review of the theory of the quasi-stationary perturbations in the atmosphere. *Meteor. Monogr.*, No. 30, Amer. Meteor. Soc., 4–19.

Sankar Rao, M., 1965: Continental elevation influence on the stationary harmonics of the atmospheric motion. *Pure Appl. Geophys.*, **60**, 141–159.

Shutts, G. J., 1978: Quasi-geostrophic planetary wave forcing. *Quart. J. Roy. Meteor. Soc.*, **104**, 331–350.

Smagorinsky, J., 1953: The dynamical influence of large-scale heat sources and sinks on the quasi-stationary mean motions in the atmosphere. *Quart. J. Roy. Meteor. Soc.*, **100**, 342–366.

Vernekar, A. D., and H. D. Chang, 1978: A statistical-dynamical model for stationary perturbations in the atmosphere. *J. Atmos. Sci.*, **35**, 433–444.

Webster, P. J., 1972: Response of the tropical atmosphere to local steady forcing. *Mon. Wea. Rev.*, **100**, 518–541.